Nanotechnology **19** (2008) 315706 (8pp) doi:10.1088/0957-4484/19/31/315706

Electromechanical actuation of single-walled carbon nanotubes: an *ab initio* study

Tissaphern Mirfakhrai[1,3], **Rahul Krishna-Prasad**[2], **Alireza Nojeh**[2] **and John D W Madden**[1]

[1] Department of Electrical and Computer Engineering and Advanced Materials and Process Engineering Laboratory, University of British Columbia, Vancouver, BC, V6T 1Z4, Canada
[2] Department of Electrical and Computer Engineering, University of British Columbia, Vancouver, BC, V6T 1Z4, Canada

E-mail: tissa@ece.ubc.ca

Received 24 January 2008, in final form 26 May 2008
Published 24 June 2008
Online at stacks.iop.org/Nano/19/315706

Abstract
The mechanical actuation of a (5, 5) single-walled carbon nanotube as a result of added charge is simulated using first-principles calculations. It is observed that while both positive and negative charging tend to expand the nanotube in the axial direction for most levels of charge, radial actuation is less even and symmetric with respect to charge. The spin distribution of the additional charges is investigated, and it is predicted that in some cases unpaired spin configurations are energetically favourable, significantly affecting actuation strains.

(Some figures in this article are in colour only in the electronic version)

1. Introduction

Carbon nanotubes (CNTs) can be thought of as rolled-up sheets of graphene with nanometre-sized diameters and lengths that have reached several millimetres. A single-walled nanotube (SWNT) consists of one such rolled-up sheet. Since the discovery of CNTs in 1991 their electronic and mechanical properties have been studied extensively, both theoretically and experimentally. Simulations and experiments have shown that CNTs are very stiff for their diameter, having Young's moduli in the TPa region [1, 2], and have tensile strengths of about 60 GPa [3], far higher than in any bulk material. It is also known that the electronic structure of CNTs depends greatly on their geometry (diameter and chirality), resulting in conducting and semiconducting CNTs of various band gaps [4].

CNTs found a new area of application when it was discovered in 1999 that they could actuate electrochemically when submersed in an electrolyte [5]. It was observed that a sheet of entangled CNTs ('Bucky paper') expands and contracts when the voltage applied to it is changed. It had been experimentally known since the 1960s [6] that the C–C bond length in ion-intercalated graphite varies when the degree of charging of the constituent graphene sheets is changed. It has been speculated that the actuation in CNTs is also the result of C–C bond length changes, rather than inter-tube effects.

A rough approximation for the change in the C–C bond length can be found by considering the Coulombic interactions between the partially-charged carbon atoms. Electrostatic forces resulting from charging the CNTs promote expansion of the CNTs due to the repulsion between the like charges. Such expansion is a quadratic function of charge. Theoretical studies were performed to relate the change in C–C bond lengths to the charge level [7, 8]. These studies predicted that, upon being charged, the CNTs may expand or contract depending on the charge type and charge level and the chirality of the CNT [9]. As had been experimentally confirmed in graphite [10], it was shown that, at small positive charge densities, the CNT can contract rather than expand, contrary to what is predicted by electrostatic considerations alone. Quantum chemical effects, such as change of the bond order and of overlap, appear to have a significant influence on the bond length as the charging is varied [8, 11].

Meanwhile, the development of new macroscopic CNT structures such as fibres [12] and yarns [13] of CNTs enabled further experimental study of their actuation. At least some

[3] Author to whom any correspondence should be addressed.

of these structures have been shown to contract [14, 15] rather than to expand, even at relatively high charge levels. This discovery makes it necessary to further investigate the mechanisms of actuation of individual CNTs. Such studies, when coupled with the geometry of the macroscopic structures, may help us understand the actuation of CNTs and pave the way for engineering applications.

In the present study, the electromechanical actuation resulting from charging a (5, 5) SWNT was investigated using *ab initio* methods in Gaussian 03 software [16]. The Hartree–Fock (HF) method was used as the method of simulation.

2. Methods

Five unit cells of the (5, 5) CNT were simulated using a 6-31G(d) basis set. The CNT was terminated by hydrogen atoms at both ends. The model consists of a total of 120 atoms. There are numerous examples in the literature where the HF method has been successfully used to explain and predict phenomena in CNTs, including bond lengths [17], which is the main quantity of interest here. The 6-31G(d) basis set used is commonly employed to model CNTs and has successfully predicted a number of properties [18, 19].

One initial concern was to know to what extent the terminating hydrogens are distorting the charge distribution over the carbon atoms. The low electron affinity of the capping hydrogen atoms leads to a partial transfer of charge between each hydrogen atom and the nearest carbon. Therefore in our analysis we set the charge on the hydrogen-bonded carbons to be equal to the sum of the charges over the C–H unit. This results in a charging level on the carbon atom that is generally consistent with those on other atoms in the nanotube.

Figure 1(a) shows a side view of the CNT structure simulated. Large grey spheres represent carbon atoms. The CNT structure is terminated with hydrogen atoms, shown as small white spheres. The system was first relaxed without extra charge to find the ground-state structure. Positive and negative charges were then added and the new relaxed configurations were found in each case, revealing the expansion or contraction of the structure. The range of charges covered spans a good portion of the range of charge levels experimentally achieved with carbon nanotubes and graphite [10].

The natural choice to study the axial actuation in a CNT would be to monitor the distance between the carbon atoms located at the two ends of the CNT structure. For this purpose, a pair of carbon atoms was taken at similar positions (with respect to the hexagonal pattern of the CNT) near the two ends of the hydrogen-terminated CNT. However, since the carbon atoms belonging to the terminal rings may be affected by edge effects to some extent, we also monitor the distance between another pair of carbon atoms further inwards along the length of the CNT to exclude the terminal rings to reduce or eliminate the edge effects. Both atom pairs are labelled in figure 1(a). The distance between these two atoms in the direction along the axis of the CNT relaxed at no charge was considered the zero-charge length of the CNT (l_0). The axial strain was calculated in per cent using $\varepsilon_1 = 100 \times \frac{\Delta l}{l_0}$, where Δl is the change in the distance between the selected pair of atoms along the axis of the CNT.

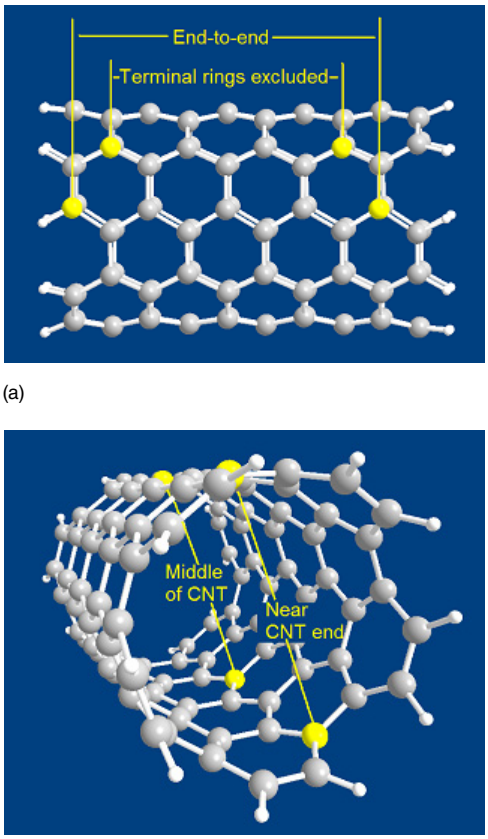

Figure 1. (a) The structure of the (5, 5) CNT simulated including the hydrogen atoms used to terminate the CNT with the location of atoms used to compute the axial strain and (b) the location of the atoms used to compute the radial strain.

In order to compute the radial strain another two pairs of carbon atoms were used. The first pair was taken near one end of the simulated structures and the second pair close to the middle of the length of the CNT, again to avoid edge effects. Each pair was selected such that the two atoms were located almost directly opposite one another across the CNT axis (figure 1(b)). Radial strain was computed as $\varepsilon_R = 100 \times \frac{\Delta R}{R_0}$, where ΔR is half the change in distance between the two carbon atoms and R_0 is half their distance before charging, used as a measure of the CNT radius.

One interesting question is how the volume of the CNT changes due to actuation. The volume of a CNT can be approximated with that of a perfect cylinder. However, we found that if no external forces were involved, the diameter of the CNT after charging would vary at different places along its length. Therefore, we decided that in order to compute the volume of the CNT, we would approximate the shape with two frusta attached on one base rather than a single cylinder (figure 2). The length of each frustum was taken as half of the end-to-end length of the CNT ($\frac{l_{CNT}}{2}$). The volume of each frustum will be $V_1 = V_2 = \frac{1}{24}\pi l_{CNT}(d_{end}^2 + d_{mid}^2 + d_{end}d_{mid})$ (see [20]) and the total volume will be $V = \frac{1}{12}\pi l_{CNT}(d_{end}^2 + d_{mid}^2 + d_{end}d_{mid})$. The distances between the atom pairs in

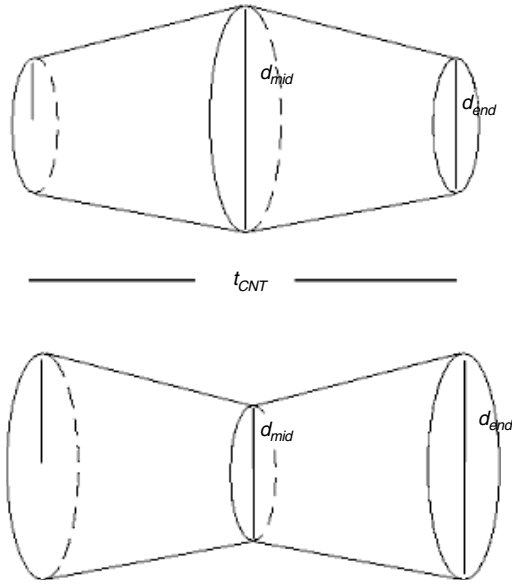

Figure 2. The volume of the CNT can be computed by approximating it with the sum of the volumes of two frusta joined at one base. The difference between d_{mid} and d_{end} and their changes are exaggerated in the image.

figure 1(b) labelled as 'Middle of CNT' and 'End of CNT' were used as the diameters of the frusta in the joint and free bases (d_{mid} and d_{end} respectively) to compute the volume.

The per cent change in the volume is computed as $\varepsilon_V = 100 \times \frac{\Delta V}{V_0}$, where ΔV is the change in the CNT volume as a result of charging, V is the volume of the CNT defined based on the frusta approximation, and V_0 is the value of V when the CNT is uncharged. No external restrictions are posed on l_{CNT}, d_{mid}, and d_{end}, and they are all free to change in our simulations.

3. Results and discussions

Figure 3 shows the strains computed using the two sets of atom pairs for the axial (a) and radial (b) directions as functions of charge. The axial strain curves in figure 3(a) show similar trends, as do the radial strains in figure 3(b) for the most part. All the same, a comparison between the two strains computed at different points along the length of the CNT shows that the electromechanical actuation is not uniform along the length of the CNT and some parts of the CNT may be shrinking (e.g., negative strain when the terminal C rings are excluded) while the overall length may be expanding. The unit of the horizontal axis is $|e|$/atom, where $|e|$ is the magnitude of the charge of an electron. In other words, the horizontal axis shows the average number of electrons per atom, with the negative sign indicating an excess of electrons. Figure 3(c) shows the change in the CNT volume as a function of charge. The volume change seems to show a less symmetric behaviour compared to the individual strain curves. Positively charged CNTs seem to have smaller volumes compared to CNTs charged with the same magnitude of charge of negative sign.

While the behaviour of all strains in figure 3 is not monotonic, the CNT generally seems to expand axially when charged either positively or negatively in an almost symmetric fashion. This is especially the case at higher charge levels. Overall the axial strain seems to increase as the charge is increased, which could be primarily due to the Coulomb-type interactions between added charges. The fluctuations to this behaviour may represent quantum effects due to redistribution of the charge at low charge levels or to artefacts due to the relatively short length of the CNT structure simulated.

In order to better understand the strains and the fluctuation patterns it is useful to look at the molecular orbitals into (from) which these electrons are being introduced (removed). Those orbitals will be the highest occupied molecular orbital (HOMO) and the lowest unoccupied molecular orbital (LUMO). Figures 4(a) and (b) illustrate the spatial distribution of some of these HOMO and LUMO orbitals as seen at small charging levels, superimposed on the middle sections (on the charge scale) of figures 3(a) and 3(b), respectively. The bean-shaped patterns represent contours of the electronic wavefunction associated with HOMO and LUMO orbitals. The red and blue portions in the online colour version indicate the positive and negative values. The shapes of the strain-to-charge plots consist of linear segments of three points for both axial and radial strains and all atom pairs considered. This behaviour can be explained by looking at the shapes of the corresponding orbitals at each point. In figure 4(a) or (b), the middle points in these segments of three, where the strain-to-charge behaviour is a straight line, are those points where the HOMO orbital is half full and therefore the HOMO and LUMO orbitals are the same. At such points an electron taken from or added to the system will be taken or added to the same spatial orbital, which would correspondingly expand or contract. However, at the points where the HOMO and LUMO have different spatial distributions, an added electron goes into a different orbital, and thus a new behaviour might be expected.

The spatial distributions of these orbitals may affect whether the tube expands or contracts in axial or radial directions in various regions of the nanotube for a given charge level. The first electrons will be taken out of the HOMO level of an uncharged CNT or added to its LUMO. As more electrons are taken out or added in, the CNT becomes charged, resulting in a slightly modified band and new HOMO and LUMO orbitals with various spatial distributions. Taking electrons out of these orbitals would lead to the expansion or contraction of the corresponding bonds. If those orbitals have a preferential directionality along the axis or along the circumference, the axial and radial strains in the CNT may be affected.

To see the overall effect of the charge in all orbitals, we can look at the total charge density on each carbon atom, which would include the effect of all lower-energy electrons in addition to those in HOMO. Figure 5 illustrates the densities of charges on each carbon atom in the system, excluding the terminating hydrogens. As can be seen from the spatial distribution of charge at various total charge levels, there are oscillation patterns, and the charge is not always uniformly distributed along the axial direction. This non-uniformity may provide an explanation for the differences between the strains computed at different positions along the length of the CNT in figure 3.

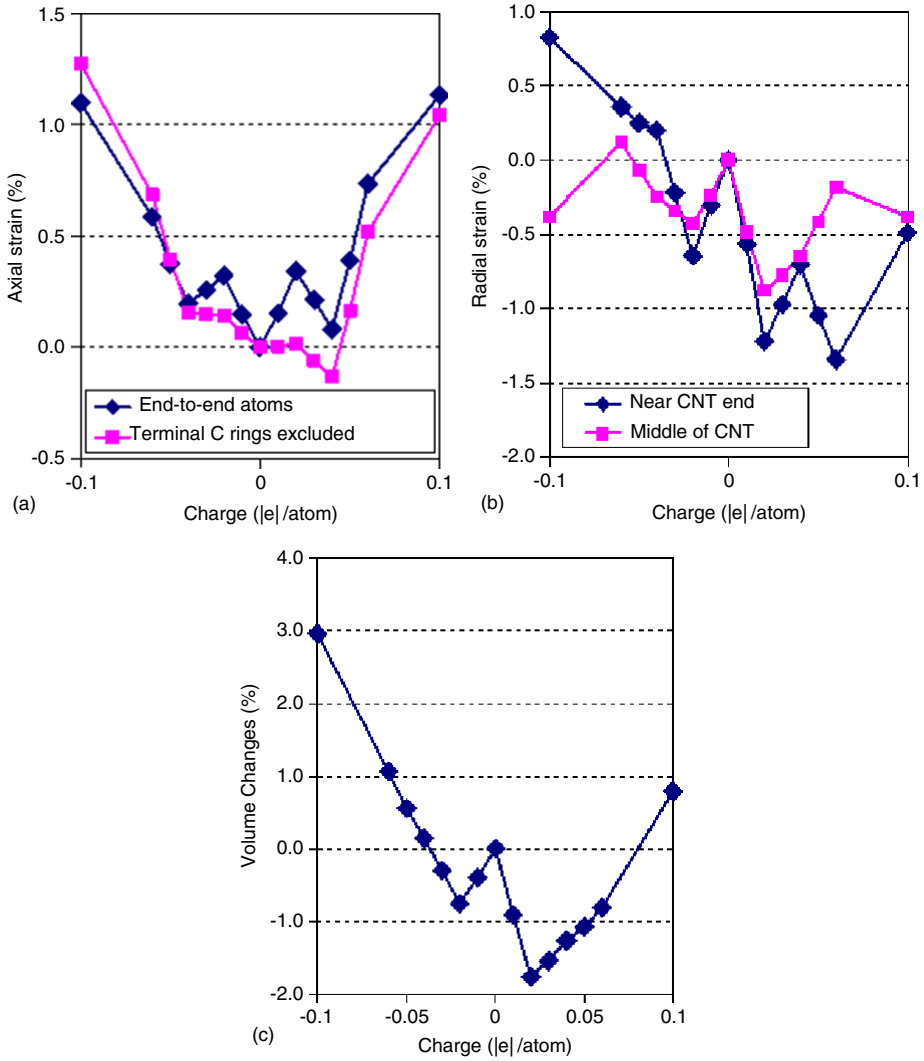

Figure 3. (a) Axial and (b) radial strains computed using the two pairs of atoms illustrated in figures 1(a) and (b), respectively. (c) Approximate CNT volume as a function of charge calculated using the frustum model.

One may argue that this non-uniformity and these oscillations arise from the fact that our model system is a very small nanotube and that the observed electron distribution is simply the 'particle-in-a-box' solution. That can be true to some extent, and also some of the extra charge over the terminal carbon rings might be due to edge effects. Ideally, we would have liked to simulate a much longer nanotube if computational resources would have allowed. However, we would like to draw the reader's attention to an important point: if a longer nanotube is used, one would need a proportionally higher amount of total charge to achieve the same level of charge per atom. In other words, the 'box' would be bigger, but the total number of particles in it would also be proportionally larger to preserve the same linear charge densities. In a three-dimensional solid-state system the interactions between electrons are often relatively weak, and thus carriers can move freely throughout. However, a CNT is a quasi-one-dimensional system in which the electrons are strongly correlated, and the interactions between electrons can play a major role [21–24]. In such systems electrons are restricted by their interactions with other electrons [25]. Due to these interactions, the total 'available space' for each electron in a longer nanotube having the same charge density may still be restricted to a small portion of the nanotube, and similar quantum confinement effects and oscillatory behaviour in the spatial charge distribution may exist. It would thus be the charge density, and not the absolute values of nanotube length and total charge, that primarily determines the quantum confinement effects and spatial charge distribution. Short nanotube models used in simulations have shown to predict various experimental results with good accuracy, and examples can be found in the literature [18, 26–28]. To study the dependence of the oscillation patterns on the CNT length, we plan to repeat some of these simulations by adding or removing a ring of carbon atoms from the CNT.

One important parameter to be considered in such molecular simulations is spin multiplicity (SM). The spin multiplicity is defined as $2S + 1$, where S is the spin quantum number, increasing by $1/2$ for every unpaired electron in the material under study. Thus if the total number of electrons in the system is even and all electrons pair up, the spin multiplicity will be 1, and if the number of electrons is odd

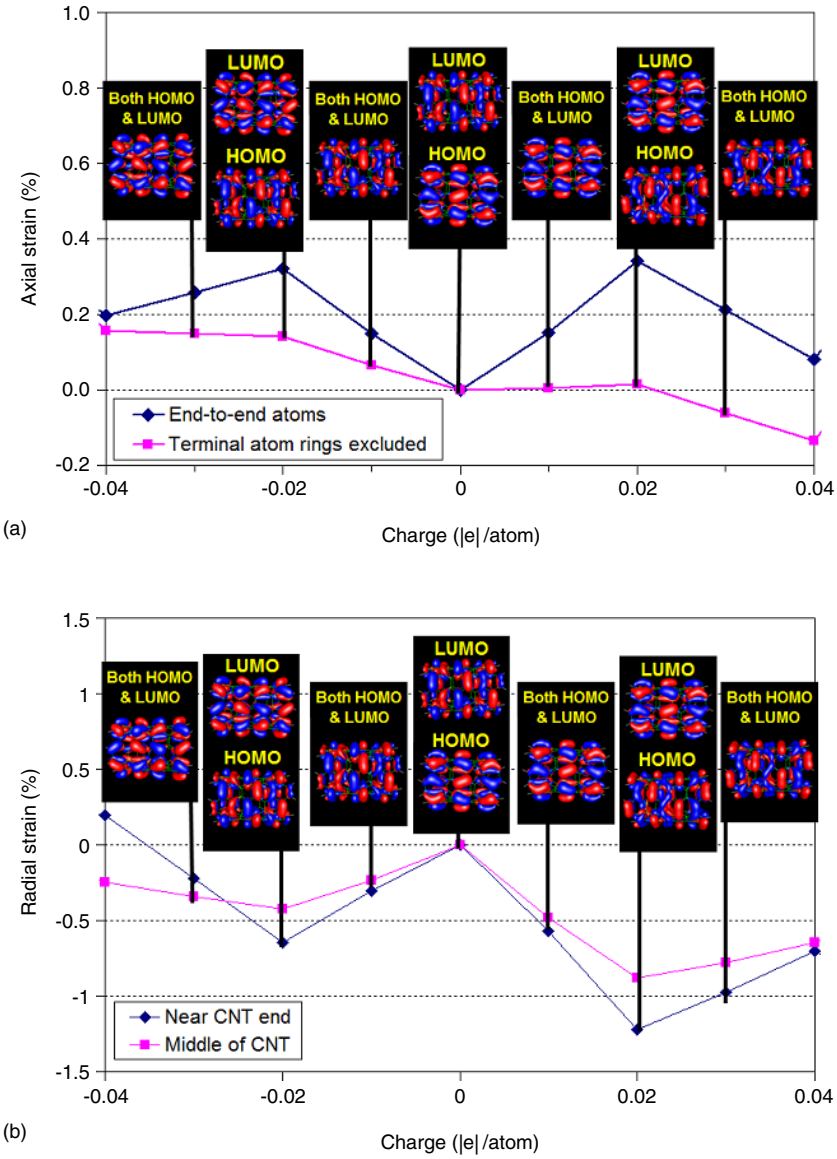

Figure 4. Spatial distributions of the highest occupied molecular orbitals (HOMOs) and the lowest unoccupied molecular orbitals (LUMOs) superimposed on the central section of the (a) axial and (b) radial strain plots (figures 3(a) and (b) respectively).

and all electrons pair up except for the last remaining electron the spin multiplicity will be 2.

Most previous studies on the electromechanical actuation of nanotubes presume that all available electrons pair up in a long-enough CNT. However, it has been shown this may not be the case in all nanotubes [29], and that large spin multiplicities may exist in some CNTs. In order to investigate this effect, each charged case studied here was simulated at a number of different spin multiplicities. This is because Gaussian, like most simulation packages, assumes a fixed spin multiplicity [16]. This way we could verify to some extent whether or not a CNT in which all available electrons pair up has a lower energy compared to one with larger spin multiplicity.

Table 1 shows the axial and radial strains at various charge levels for two different spin multiplicities. For the first set it has been assumed that all available electrons pair up, resulting in spin multiplicities of either 1 or 2. In the second data set, it has been assumed that none of the extra electrons pair up, and so the spin multiplicity has been set to the number of added charges plus one. As can be seen from table 1, the difference in strains at different spin multiplicities is significant (reaching 0.9% for radial strain and 0.33% for axial strain) and of the same order of magnitude as the strain values themselves. Therefore it is important to find which values of spin multiplicity correspond to the ground state of the material. In order to further investigate the issue, we computed the total system energy as a function of the spin multiplicity. This energy includes the nuclei–nuclei interaction, electron–electron interaction, nuclei–electron interaction and the kinetic energy of the electrons. The change in total system energy for an uncharged CNT is plotted versus the spin multiplicity value in figure 6. For the uncharged CNT, it seems that a spin multiplicity of 1 (all electrons paired) indeed results in

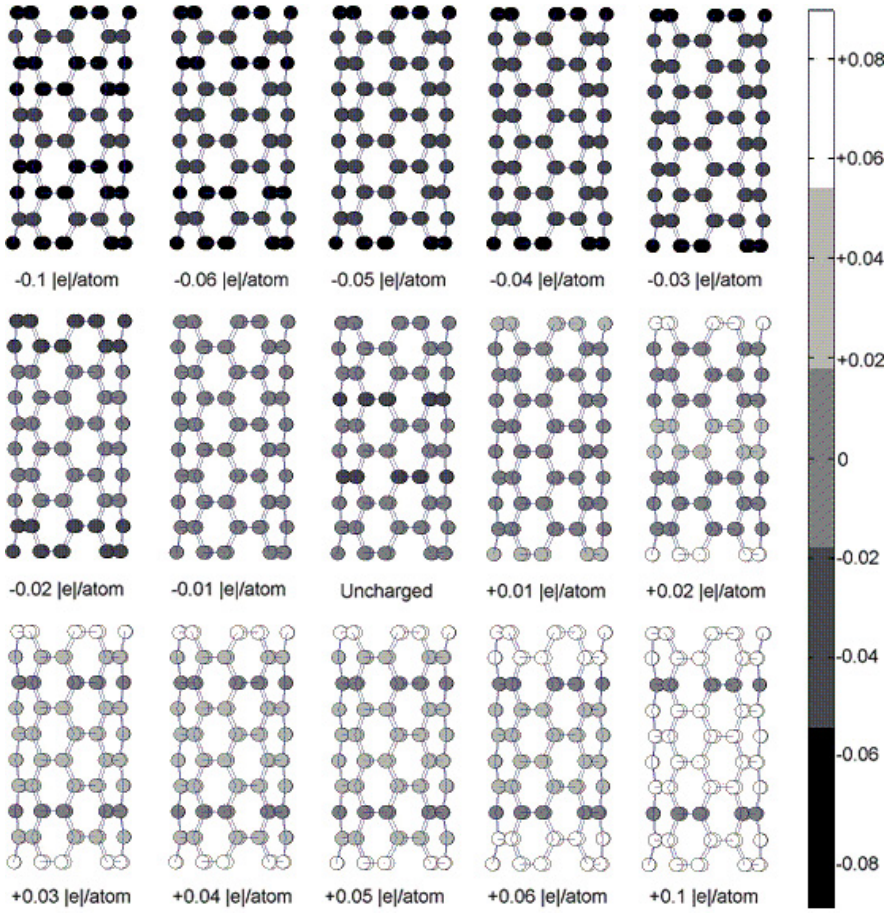

Figure 5. Total charge density distribution at different charge levels.

Table 1. Effect of spin multiplicity (SM) on the axial and radial strain in a (5, 5) CNT.

	Axial			Radial		
Charge ($\|e\|$/atom)	ε_A (%) at SM = 1 or 2	ε_A (%) at SM = $\|q\|+1$	$\Delta\varepsilon_A$ (%)	ε_R (%) at SM = 1 or 2	ε_R (%) at SM = $\|q\|+1$	$\Delta\varepsilon_R$ (%)
0.06	0.735	0.577	0.158	−1.342	−0.437	0.905
0.05	0.393	0.223	0.170	−1.047	−0.507	0.540
0.03	0.213	0.288	0.075	−0.975	−0.784	0.192
0.02	0.342	0.009	0.333	−1.221	−0.390	0.831
0.01	0.152	0.152	0.000	−0.568	−0.568	0.000
0.000	0.000	0.000	0.000	0.000	0.000	0.000
−0.01	0.149	0.149	0.000	−0.307	−0.307	0.000
−0.02	0.321	0.064	0.257	−0.646	0.054	0.699
−0.03	0.258	0.228	0.031	−0.219	0.098	0.317
−0.05	0.375	0.345	0.030	0.247	0.639	0.391
−0.06	0.586	0.504	0.082	0.356	0.819	0.464

the lowest energy among the values considered. Based on our simulations for various charge levels (not all shown here), this pattern seems to hold for most of the charged CNTs. However at two of the charge values considered, interesting exceptions were found. The inset in figure 6 shows the total system energy for CNTs with charge levels of $-0.1|e|$/atom (a total of 10 electrons added) and $+0.1|e|$/atom (a total of 10 electrons removed). It can be seen that the total system energies have their minima at spin multiplicity values of 9 and 7, respectively, rather than 1. This means that some of the electrons must remain unpaired in the ground state, which could indicate possible magnetic effects in the CNT. The strain values in figure 3 are therefore obtained using the spin multiplicity values that among those we have tried have given the lowest energy levels.

Comparing the total system energies for different spin multiplicities at different charge levels (figure 7) implies that the pairing of all available electrons may result in the lowest

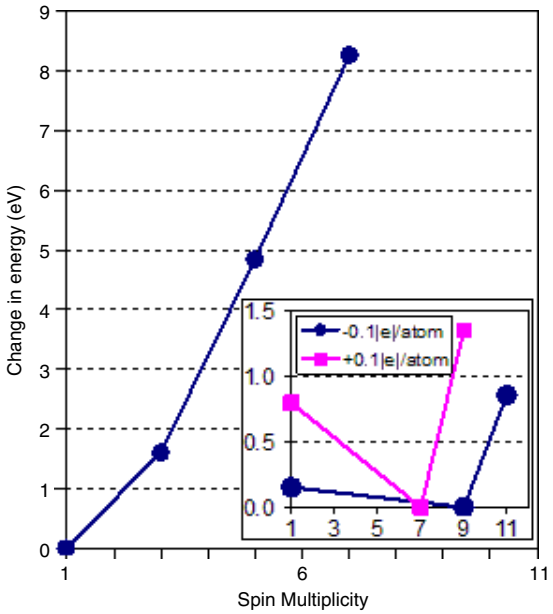

Figure 6. The change in the total system energy for an uncharged CNT as a function of its spin multiplicity. The inset plot shows the change in total system energy for the same CNT charged to $\pm 0.1|e|$/atom. The minimum energy value has been taken to be zero for each curve. These base values are -103.36 keV in the main plot and -103.25 and -103.2 keV for $+0.1$ and $-0.1|e|$/atom, respectively, in the inset. The lines are added only to help visually.

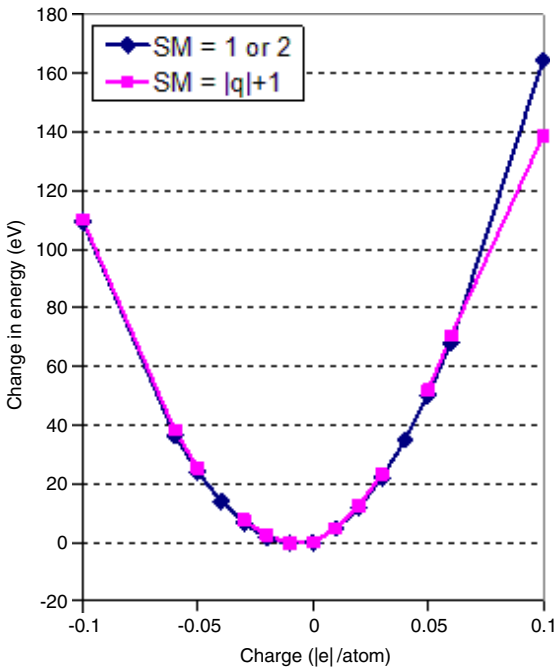

Figure 7. The change in total system energy as a function of charge at two different spin multiplicities. The minimum total system energy of -103.36 keV has been subtracted from all data points. Note that as demonstrated by figure 6, at $\pm 0.1|e|$/atom the minimum energy occurs at a spin multiplicity other than those plotted here.

total energy at all charge levels studied, with the exception of the $-0.1|e|$/atom and $+0.1|e|$/atom charge cases. This observation supports our use of spin multiplicities of 1 and 2 in computations of the axial and radial strains discussed earlier.

A number of other works have addressed the issue of electromechanical actuation of single nanotubes. Results for axial strains in a (5, 5) CNT from a few relevant papers are compared in figure 8. Our results (connected by lines in the figure) are in qualitative agreement with the strains computed for a (5, 5) CNT by Verissimo-Alvez *et al* in [11] using tight-binding theory (squares). Both results predict a small axial contraction at small values of positive charge, although this happens at different charge levels in the two models. A direct comparison between our results and those in [11] is not possible because their plot for a (5, 5) CNT spans a much smaller range of charge values than ours. Tight-binding theory is not as accurate as HF. However, the computational loads required for tight binding are much reduced because of the rougher approximations employed. This provides the possibility of simulating long CNTs. Our simulations provide more accurate data about shorter CNTs. Therefore, the two approaches are complementary, and both provide useful information to help understand the electromechanical actuation behaviour of CNTs. Results for radial strains were not presented in [11].

A more comparable paper to the present work is by Ghosh *et al* [30] (circles), obtained using restricted HF calculations using the GAMESS package [31]. They have simulated five unit cells of the (5, 5) CNT as we have, and their results for axial strain are in good agreement with our end-to-end

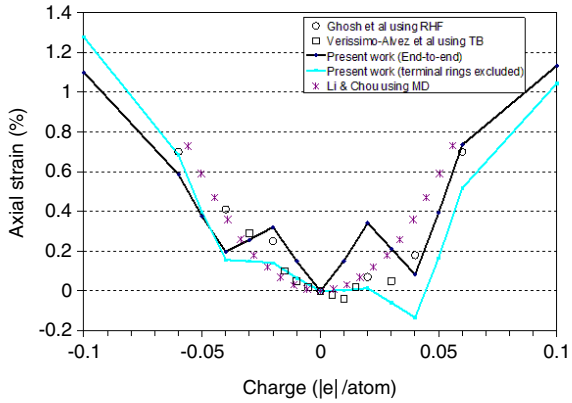

Figure 8. Comparison of axial strain results of the present study with those of Ghosh *et al* [30], Verissimo-Alvez *et al* [11], and Li and Chou [32].

strain results. Their charge resolution is lower than ours, and therefore it cannot be directly used to support the effect of the filling of the orbitals on strain shown in figure 4. However, they allow the charge to transfer to the CNT from atoms outside it, which is a step towards simulating conditions closer to those in actuation experiments.

Another relevant study is by Li and Chou [32], in which a uniform charge distribution has been assumed over all carbon atoms (asterisks). A molecular structural mechanics method based on the Amber [33] molecular force field is employed. This approach is classical, and does not include the quantum effects such as the fact that electrons exist in orbitals with diverse and non-trivial spatial distributions. As a result none

of the contraction effects have been observed, and the CNT was seen to expand quadratically as a function of charge at all charge levels.

In general, the strains predicted by all of the above models are in the same order of magnitude, and qualitatively all models predict similar behaviour with a tendency of strains to increase as charge levels are increased. Tight-binding and classical molecular dynamics approaches employ simpler levels of theory that make it possible to simulate much longer CNT structures at the expense of accuracy. Approaches like that of [32] do not allow for charge redistribution, which may affect their results significantly. We have shown that it is necessary to consider the effect of spin multiplicity to obtain the minimum energy state and the correct strain value.

4. Conclusions

The dependence of the dimensions and volume of an SWNT on its charge level was studied. It was observed that while charging (both positive and negative) almost always leads to an axial expansion of the nanotube, certain levels of positive charging can lead to contraction. A relationship between the dimensional change and the degree of molecular orbital filling was observed. The effect of spin multiplicity on strain was studied for the first time, and it was shown that in some cases states with unpaired spins are more energetically favourable. The spin multiplicity can have a significant effect on the actuation strains, and future work in this area should explore it further.

Acknowledgments

The authors wish to thank the Natural Sciences and Engineering Research Council of Canada for their support, especially in the form of the Undergraduate Student Research Award granted to RKP. They would also wish to thank Dr Peyman Servati for his insightful advice on the orbital and band structure of materials, and the Gaussian technical support staff, especially Dr Fernando R Clemente, for their timely help with Gaussian simulation issues.

References

[1] Liu T T and Wang X 2006 *Phys. Lett.* A **365** 144–8
[2] Dai X B, Merlitz H and Wu C X 2006 *Eur. Phys. J.* D **54** 109–12
[3] Baughman R H, Zakhidov A A and de Heer W A 2002 *Science* **297** 787–92
[4] Avouris P, Appenzeller J, Martel R and Wind S J 2003 *Proc. IEEE* **91** 1772–84
[5] Baughman R H *et al* 1999 *Science* **284** 1340–4
[6] Nixon D E and Parry G S 1969 *J. Phys. C: Solid State Phys.* **2** 1732
[7] Chan C T, Kamitakahara W A, Hoand K M and Eklund P C 1987 *Phys. Rev. Lett.* **58** 1528–31
[8] Pietronero L and Strässler S 1981 *Phys. Rev. Lett.* **47** 593–96
[9] Gartstein Y N, Zakhidov A A and Baughman R H 2003 *Phys. Rev.* B **68** 115415
[10] Sun G, Kurti J, Kertesz M and Baughman R H 2002 *J. Am. Chem. Soc.* **124** 15076–80
[11] Verissimo-Alves M, Koiller B, Chacham H and Capaz R B 2003 *Phys. Rev.* B **67** 161401
[12] Vigolo B, Penicaud A, Coulon C, Sauder C, Pailler R, Journet C, Bernier P and Poulin P 2000 *Science* **290** 1331–4
[13] Zhang M, Atkinson K R and Baughman R H 2004 *Science* **306** 1358–61
[14] Mirfakhrai T, Oh J, Kozlov M, Fok E C W, Zhang M, Fang S, Baughman R H and Madden J D W 2007 *Smart Mater. Struct.* **16** S243
[15] Kozlov M, Zhang M, Fang S, Mirfakhari T, Madden J D and Baughman R H 2005 Electro-mechanical actuation of carbon nanotube yarns and sheets *Materials Research Society Fall Meeting (November 2005)*
[16] Frisch M J *et al* 2004 *Gaussian 03, Revision C.02* (Wallingford, CT: Gaussian)
[17] Szabo A and Ostlund N S 1996 *Modern Quantum Chemistry: Introduction to Advanced Electronic Structure Theory* (Mineola, NY: Dover)
[18] Nojeh A, Shan B, Cho K and Pease R F W 2006 *Phys. Rev. Lett.* **96** 056802
[19] Won C Y, Joseph S and Aluru N R 2006 *J. Chem. Phys.* **125** 114701–1
[20] Harris J W and Stocker H 1998 *Handbook of Mathematics and Computational Science* (New York: Springer) p 105
[21] Balents L and Fisher M P A 1997 *Phys. Rev.* B **55** 973–6
[22] Saito R, Dresselhaus G and Dresselhaus M S 1998 *Physical Properties of Carbon Nanotubes* (London: Imperial College Press)
[23] Krotov Y A, Lee D-H and Louie S G 1997 *Phys. Rev. Lett.* **78** 4245–8
[24] Kane C, Balents L and Fisher M P A 1997 *Phys. Rev. Lett.* **79** 5086–9
[25] Giamarchi T 2004 *Quantum Physics in One Dimension* (Oxford: Clarendon) p 440
[26] Luo J, Peng L M, Xue Z Q and Wu J L 2002 *Phys. Rev.* B **66** 155407
[27] Zhou G, Duan W and Gu B 2001 *Phys. Rev. Lett.* **87** 095504
[28] Kim C, Kim B, Lee S M, Jo C and Lee Y H 2002 *Phys. Rev.* B **65** 165418
[29] Mestechkin M M 2006 *Physica* B **382** 305–11
[30] Ghosh S, Gadagkar V and Sood A K 2005 *Chem. Phys. Lett.* **406** 10–4
[31] Schmidt M W *et al* 1993 *J. Comput. Chem.* **14** 1347–63
[32] Li C-Y and Chou T-W 2006 *Nanotechnology* **17** 4624–8
[33] Pearlman D A, Case D A, Caldwell J W, Seibel G L, Singh U C, Weiner P A and Kollman P A 1991 *AMBER 4.0* San Francisco, CA (UCSF) Department of Pharmaceutical Chemistry, University of California